Chemistry & Biology, Vol. 9, 1247–1255, November, 2002, ©2002 Elsevier Science Ltd. All rights reserved. PII S1074-5521(02)00263-6

Stereoselectivity of Enoyl-CoA Hydratase Results from Preferential Activation of One of Two Bound Substrate Conformers

Alasdair F. Bell,[1] Yuguo Feng,[1] Hilary A. Hofstein,[1] Sapan Parikh,[1] Jiaquan Wu,[1] Michael J. Rudolph,[2] Caroline Kisker,[2] Adrian Whitty,[3] and Peter J. Tonge[1,4]

[1]Department of Chemistry
[2]Department of Pharmacological Sciences
Center for Structural Biology
SUNY at Stony Brook
Stony Brook, New York 11794
[3]Department of Drug Discovery
Biogen, Inc.
Cambridge, Massachusetts 02142

Summary

Enoyl-CoA hydratase catalyzes the hydration of *trans*-2-crotonyl-CoA to 3(*S*)- and 3(*R*)-hydroxybutyryl-CoA with a stereoselectivity (3(*S*)/3(*R*)) of 400,000 to 1. Importantly, Raman spectroscopy reveals that both the *s-cis* and *s-trans* conformers of the substrate analog hexadienoyl-CoA are bound to the enzyme, but that only the *s-cis* conformer is polarized. This selective polarization is an example of ground state strain, indicating the existence of catalytically relevant ground state destabilization arising from the selective complementarity of the enzyme toward the transition state rather than the ground state. Consequently, the stereoselectivity of the enzyme-catalyzed reaction results from the selective activation of one of two bound substrate conformers rather than from selective binding of a single conformer. These findings have important implications for inhibitor design and the role of ground state interactions in enzyme catalysis.

Introduction

Enoyl-CoA hydratase (crotonase) is the second enzyme in the β-oxidation pathway and catalyzes the *syn* hydration of α,β-unsaturated-CoAs (Figure 1A) [1]. V/K for the hydration of crotonyl-CoA is close to the diffusion-controlled limit for the reaction, and a primary goal of our research is to dissect the molecular events that result in an enzyme-catalyzed rate increase of greater than 10^{11} compared to the uncatalyzed reaction [2]. The enzyme is the eponymous member of the crotonase superfamily in which the primary conserved feature is a common protein fold that produces an oxyanion hole used to stabilize carbanionic transition states [3, 4]. In all the family members that have so far been crystallized, one of the oxyanion hydrogen bond donors lies at the N terminus of an α helix. In enoyl-CoA hydratase the backbone amide groups of A98 and G141 constitute the oxyanion hole, and structural studies have also revealed the presence of two potential catalytic glutamates (E144 and E164) that bind the catalytic water molecule [5–7]. Site-directed mutagenesis and enzyme kinetics have demonstrated that the two glutamates act together to catalyze the concerted addition of water, and replacement of either residue with glutamine results in a dramatic (10^4- to 10^6-fold) reduction in k_{cat} [8–13]. Additionally, the replacement of G141 with proline, which specifically removes a hydrogen bond donor in the oxyanion hole, also results in a 10^6-fold reduction in k_{cat} [14].

Raman spectroscopy has been used extensively to probe the activation of ligands by enoyl-CoA hydratase [14–16]. The ligand of choice for these studies has been a substrate analog, hexadienoyl-CoA (HD-CoA; Figure 1B), in which an extra conjugated double bond thermodynamically stabilizes the ligand. With the aid of extensive isotope labeling, normal mode calculations, and model compound studies, a clear picture of the vibrational spectrum of HD-CoA has been developed [14, 16], resulting in a powerful probe of the intimate details of enzyme catalysis. The analysis of the vibrational spectrum has focused on the double bond stretching region (1500–1700 cm^{-1}) where the position of bands reflects a combination of the distribution of electrons within the double bonds and the vibrational coupling between the two C=C bonds and the carbonyl group. For enoyl-CoA hydratase, the changes in Raman band positions that occur upon binding to the enzyme reflect ligand polarization resulting from a reduction in bond order of the carbonyl group and subsequent alteration in the vibrational coupling throughout the molecule. In particular, the enzyme selectively decouples the conjugated hexadienoyl group so that the terminal C4=C5 double bond is no longer vibrationally coupled to the remainder of the molecule, and a new mode localized on the C3=C2-C1=O enone fragment appears. We are particularly interested in understanding the structural basis for ligand polarization in order to determine the role that enzyme-substrate interactions play in substrate activation and transition state stabilization.

Since the polarizing effect of the enzyme on HD-CoA was eliminated by mutating one of the residues constituting the oxyanion hole (G141P) [14], and given that the active site remains intact in this mutant according to X-ray crystallography (unpublished data), the hydrogen bonding network generated by the oxyanion hole around the carbonyl oxygen of HD-CoA is clearly important in ligand polarization. In the current study we have extended our structure-function studies to include four active site mutants in which the catalytic glutamates have been replaced by either aspartate or glutamine. These mutants and the wild-type enzyme span a 10^6-fold range of k_{cat} and the effect of mutagenesis on polarization of HD-CoA has been explored using Raman spectroscopy. Our results provide a structural basis for the observed stereoselectivity of the reaction. Specifically, enoyl-CoA hydratase binds two distinct substrate conformers, both of which may be hydrated to give different product enantiomers, but selectively activates only one conformer to hydration. Preferential hydration

[4]Correspondence: peter.tonge@sunysb.edu

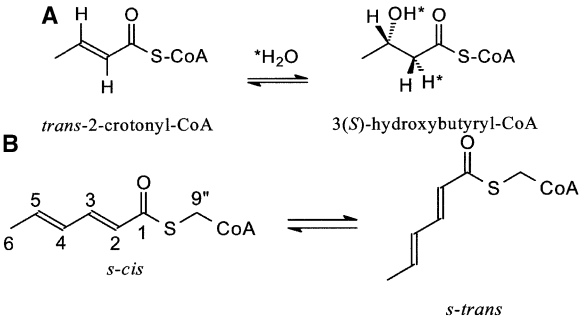

Figure 1. Reaction Catalyzed by Enoyl-CoA Hydratase and Structure of Hexadienoyl-CoA

(A) Reaction catalyzed by enoyl-CoA hydratase.

(B) Numbering scheme for hexadienoyl-CoA and the *s-cis* and *s-trans* conformers.

of the activated substrate conformer produces the observed stereochemical outcome of the reaction.

Results and Discussion

Raman Spectra of Wild-Type and Mutant Enoyl-CoA Hydratases Provide Evidence for More than One Bound Conformer of HD-CoA

The difference Raman spectra of HD-CoA in aqueous solution and bound to wild-type and four mutants of enoyl-CoA hydratase (E144Q, E144D, E164D, and E164Q) are displayed in Figure 2A. The wave number and intensity data together with the vibrational assignments for the major bands in the double bond stretching region (1500–1700 cm^{-1}) of HD-CoA are summarized in Table 1. For HD-CoA in solution, three C=C stretching bands can be resolved, indicating the presence of two conformers, which have been identified as *s-cis* and *s-trans* around the C1-C2 single bond (Figure 1B) [14]. Upon binding to wild-type enoyl-CoA hydratase, the Raman bands associated with the C=C stretching modes are altered, reflecting a change in their normal mode compositions relative to the ligand in solution (Table 1). These changes have previously been interpreted to indicate (1) that the enzyme preferentially binds the *s-cis* HD-CoA conformer and (2) that the enzyme polarizes the hexadienoyl ground state, uncoupling the terminal C4=C5 bond (1640 cm^{-1} band) and polarizing the C3=C2-C1=O enone fragment (1565 cm^{-1} band) [14]. These polarizing forces in the active site are expected to activate the substrate to catalysis and reflect the forces in place to stabilize the carbanionic transition state.

It is clear from Table 1 and Figure 2A that there are only minor modifications (less than 5 cm^{-1}) in the positions of the two double bond stretching bands near 1640 and 1565 cm^{-1} for the wild-type and mutant enzymes. Thus, the observed changes in vibrational coupling within the hexadienoyl moiety upon binding to enzyme *are not* dependent on either of the two catalytic glutamates (E144 and E164). However, despite the similarity in band positions, the Raman spectra of the E144 and E164 mutants do exhibit one important difference relative to the wild-type spectrum. Due to a reduction in the intensity of the two bands at 1640 and 1565 cm^{-1}, two new bands, at about 1630 and 1595 cm^{-1}, are clearly evident in the difference spectra of the mutants that are not well resolved in the wild-type spectrum (Figures 2A and 2B). Under the conditions employed for the Raman measurements, we calculate that 94% of the HD-CoA is bound to the enzyme; therefore, the additional bands cannot be attributed to the presence of free HD-CoA. Since only two C=C stretching bands are expected for a single conformer of HD-CoA, the presence of four bands provides strong evidence for two distinct conformations of HD-CoA bound to the enzyme.

The identity of the two bound conformers can be obtained from the Raman spectra by comparison with model compounds. Normal mode calculations have shown that the conformation around the C1-C2 single bond of the hexadienoyl group can have a strong influ-

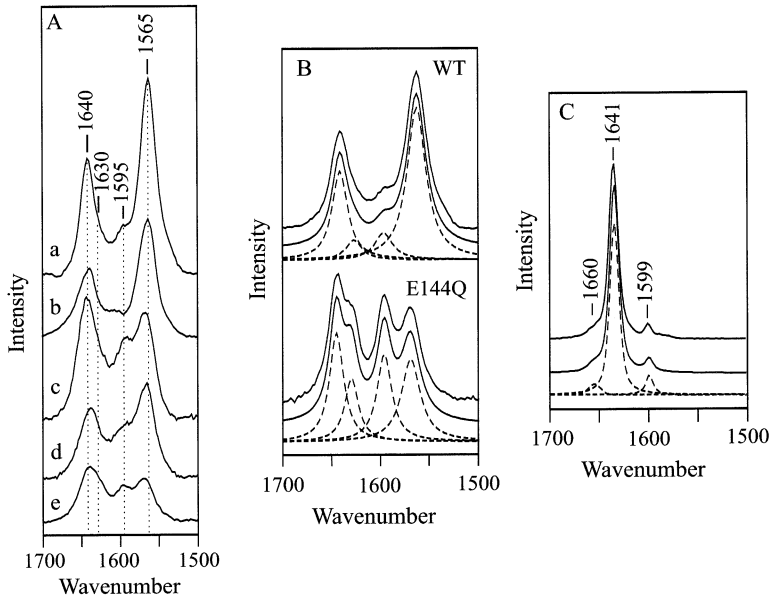

Figure 2. Evidence for Two Bound Conformers from the Raman Spectra of Hexadienoyl-CoA Bound to Enoyl-CoA Hydratase

(A) Raman spectra of HD-CoA bound to (a) wild-type, (b) E144D, (c) E164D, (d) E164Q, and (e) E144Q enoyl-CoA hydratases. The concentration of enzymes were between 0.8 and 1 mM, and 0.8 equivalents of HD-CoA were added in each case.

(B) Curve fitting of HD-CoA bound to wild-type (wt) and E144Q enoyl-CoA hydratases using Win-IR software. The E144Q spectrum had a reduced slit width to produce a higher resolution spectrum for curve fitting and is thus slightly different from that displayed in (A). The top trace is the raw spectrum while the lower solid black and dashed traces are the results of curve fitting.

(C) Raman spectrum obtained from a single crystal of *S*-hexadienoyl-*N*-acetylcysteamine. 100 mW 752 nm laser radiation, 1 min data collection time. The top trace is the experimental spectrum while the solid black and dashed traces are the results of curve fitting.

Table 1. Raman Band Positions and Intensity Together with Band Assignments for HD-CoA Bound to Enoyl-CoA Hydratase

Enzyme	Position[a] (Intensity)	Position[a] (Intensity)	Position[a] (Intensity)	Position[a] (Intensity)
wt	1640 (59)	1627 (16)	1597 (26)	1565 (100)
E144Q	1642 (28)	1628 (17)	1595 (23)	1568 (21)
E144D	1640 (35)	1629 (14)	1594 (22)	1565 (60)
E164Q	1643 (35)	1626 (16)	1595 (27)	1567 (48)
E164D	1644 (58)	1629 (17)	1595 (29)	1567 (56)
Raman	*s-cis*	*s-trans*	*s-trans*	*s-cis*
Assignment[b]	C4=C5	C4=C5+C1=O1	C2=C3	C2=C3+C1=O1

[a] Position and intensity data determined from deconvoluted Raman spectra. The Raman intensity data are corrected for laser power and are estimated to be accurate to ±10%. Intensities are normalized with respect to the 1565 cm^{-1} band in wild-type enzyme.
[b] Raman band assignments reflect the predominant bond contributions as determined by isotope labeling and normal mode calculations [14].

ence on the position of the C=C stretching modes due to changes in the degree of vibrational coupling with the carbonyl group [14, 17]. In aqueous solution at room temperature, both *s-cis* and *s-trans* conformers are populated and consequently the Raman spectra of hexadienoyl model compounds at this temperature contain bands associated with both conformers. In order to provide unambiguous band assignments, we have analyzed Raman data obtained under experimental conditions in which only the *s-cis* or *s-trans* conformers are present. Since the *s-cis* conformer is thermodynamically more stable, lowering the temperature will selectively enrich this population, and indeed, an earlier low-temperature Raman study identified the bands due to *s-cis* hexadienoyl-ethyl thioester conformer [16, 17]. Additionally, we have observed that the model compound HD-NAC crystallizes in the *s-trans* conformer (data not shown). The Raman spectrum obtained from a single crystal of HD-NAC between 1500 and 1700 cm^{-1} is shown in Figure 2C. Curve fitting reveals three bands in the double bond stretching region at 1660, 1641, and 1599 cm^{-1}. The weak band at 1660 cm^{-1} can be assigned to the C=O stretching frequency of the hexadienoyl moiety. The two bands at 1641 and 1599 cm^{-1} correspond to the in-phase and out-of-phase combinations of the two C=C stretching coordinates that are also coupled to the C=O stretch. Based on their relative intensities, the band at 1641 cm^{-1} is assigned to the in-phase combination, whereas the 1599 cm^{-1} band is assigned to the out-of-phase combination. Taking the *s-cis* and *s-trans* model compound spectra together, we have assigned the bands in the enoyl-CoA hydratase mutants near 1640 and 1565 cm^{-1} to the *s-cis* conformer and the bands near 1630 and 1595 cm^{-1} to the *s-trans* conformer of the hexadienoyl group bound to the enzyme. Closer inspection and curve fitting of the wild-type data reveals that the additional bands at 1630 and 1595 cm^{-1}, prominent in the Raman spectra of HD-CoA bound to the mutants, are also present in the Raman spectrum of HD-CoA bound to wild-type enzyme (Figure 2B). This indicates that the wild-type enzyme is also able to bind two conformers. An earlier Raman study on HD-CoA binding to wild-type enoyl-CoA hydratase [14] did not observe additional bands due to a second conformer. However, we note that the experimental conditions were somewhat different in this study and that the bands from the *s-trans* conformer are relatively weak in the wild-type spectrum.

The intensity of the bands near 1565 and 1640 cm^{-1}, assigned to the *s-cis* conformer, decrease dramatically for the E144Q and E164Q mutants relative to the wild-type enzyme, whereas the *s-trans* marker bands remain relatively constant (Table 1). In general, under nonresonance conditions Raman band intensities are determined by changes in molecular polarizability caused by displacement of the atoms during the vibration and are fundamentally related to the electrooptical properties of the constituent atoms and bonds. This is manifested in an exquisite sensitivity for the Raman band intensities to the distribution of charge in the molecule being studied [18]. The intensity changes that we observe may reflect subtle effects on the ground and/or excited states of HD-CoA due to its interactions with the two ionizable side chains of E144 and E164. However, we note that the band positions, which are sensitive to ground state changes, are only slightly shifted in the mutants, leading us to conclude that excited state effects dominate. Regardless of the origin of the intensity changes, the key observation is that the Raman bands due to the *s-cis* conformer are considerably weaker in the mutants, revealing the bands attributable to the *s-trans* conformer.

X-Ray Crystallographic and Modeling Studies

In order to supplement the Raman studies with additional structural information, we have determined the 2.1 Å X-ray crystal structure of HD-CoA bound to enoyl-CoA hydratase (Protein Data Bank code 1MJ3) (Table 2). In agreement with previous ligand bound structures [5–7], the hexadienoyl carbonyl group is hydrogen bonded to the backbone amide groups of A98 and G141. In addition, a water molecule forms hydrogen bonds to the two catalytic glutamates (E144 and E164) and is optimally positioned to nucleophilically add to the C3 hexadienoyl carbon (Figure 3A). The bound hexadienoyl group is *s-cis* about the C1-C2 single bond and, as discussed previously [5–7, 19], this orientation of the substrate will yield the 3(*S*)-hydroxyacyl product.

Our Raman studies indicate that the *s-cis* and *s-trans* HD-CoA conformers are exposed to substantially different polarizing forces in the active site of enoyl-CoA hydratase. However, there is no evidence in the X-ray structure of HD-CoA bound to enoyl-CoA hydratase for the *s-trans* HD-CoA conformer. This likely reflects the fact that the X-ray data were collected at 100 K, at which temperature only the *s-cis* conformer will be populated even in solution, and could also result from differences

Table 2. Data Collection and Refinement Statistics

Data Collection	
Space group	$P2_12_12_1$
Unit cell dimensions: a, b, c (Å)	76.9, 95.2, 249.4
Number of unique reflections	97,058
Resolution limits (Å)	50–2.1
Redundancy	4.2
Completeness[a] (%)	90.1 (78.5)
R_{sym}[b] (%)	7.9 (43.3)
$<I> / <\sigma I>$[c]	16.3 (2.4)
Refinement Statistics	
Number of reflections used / free	92,257 / 4,801
Number of protein / ligand / solvent atoms	11,868 / 273 / 920
R_{cryst} (R_{free})[d] (%)	17.9 (22.9)
Deviations from ideal values in:	
Bond distances (Å)	0.02
Bond angle (°)	3.0
Planar 1,4 distances (Å)	0.013
Chiral volumes (Å^3)	0.18
Torsion angles (Å)	5.3
Van der Waals repulsion (Å)	0.26
Ramachandran statistics[e]	90.5 / 9.5
B factor all atoms / ligand[f] (Å^2)	29 / 36
Overall coordinate error[g] (Å)	0.19

[a] Numbers in parentheses refer to the respective highest resolution data shell in each data set.

[b] $R_{sym} = \Sigma_{hkl}\Sigma_i|I_i - <I>|/\Sigma_{hkl}\Sigma_i I_i$ where I_i is the i^{th} measurement and $<I>$ is the weighted mean of all measurements of I.

[c] $<I> / <\sigma I>$ indicates the average of the intensity divided by its average standard deviation.

[d] $R_{cryst} = \Sigma_{hkl}||F_o| - |F_c||/\Sigma_{hkl}|F_o|$ where F_o and F_c are the observed and calculated structure factor amplitudes. R_{free} is the same as R_{cryst} for 5% of the data randomly omitted from refinement.

[e] Ramachandran statistics indicate the fraction of residues in the most favored and additionally allowed regions of the Ramachandran diagram as defined by PROCHECK [57]. No residues are in disallowed regions.

[f] B factor refers to temperature factor for all atoms and for ligand structure.

[g] Overall coordinate error estimated from R_{free}.

in other experimental conditions. While vibrational spectroscopy provides a snapshot of all structures present at any instant, X-ray crystallography will only provide information on conformers that are substantially populated. Consequently, modeling studies were performed using the crystal structure as a starting point, which revealed that the *s-trans* conformer can be accommodated in the active site either by relocation of the hexadienoyl tail or by repositioning of the carbonyl group. Since the carbonyl group is hydrogen bonded to the backbone amides of G141 and A98 in the *s-cis* conformer, it is possible that this favorable interaction may persist in the *s-trans* conformer as shown in Figure 3B. In addition, the fact that the G141P and A98P mutants do not form any appreciable 3(*R*)-hydroxybutyryl-CoA supports the hypothesis that the substrate conformer that leads to the 3(*R*) product enantiomer is hydrogen bonded to these residues in the active site [20]. However, there is a large wave number shift (1595 to 1565 cm^{-1}) and decoupling of the terminal double bond for the *s-cis* conformer, whereas for the *s-trans* conformer there are much smaller shifts (1640 to 1630 cm^{-1} and 1602 to 1595 cm^{-1}) and no decoupling of the C4=C5 stretching modes on binding. If the hydrogen bonding interactions are similar in both conformers, then additional active site interactions must be involved in ligand polarization. It is clear from the modeling studies that *s-cis* to *s-trans* isomerization will alter the alignment of the hexadienoyl group with respect to the active site α helix (Figure 3), and this may partially account for the observed differences in the vibrational spectra of the two bound conformers. This α helix is likely conserved through the crotonase superfamily, and similar importance has been attached to the analogous helix in 4-chlorobenzoyl-CoA dehalogenase, where ligand polarization and catalysis are also intimately linked [21–24]. A similar explanation has been advanced for the differences observed in the Raman spectra of 5-methylthienylacryloyl (5MTA) chromophore conformers bound in the active site of thiol- and selenol-subtilisin [25].

Stereoselectivity of the Enzyme-Catalyzed Reaction Is Controlled by Preferential Hydration of One of Two Bound Conformers

The observation of two bound conformers has important implications for the stereoselectivity of the enoyl-CoA hydratase-catalyzed reaction. The hydration of *trans*-2-crotonyl-CoA stereospecifically produces the 3(*S*)-hydroxybutyryl-CoA enantiomer; however, it has been found that the 3(*R*)-enantiomer is also formed, but only once in every 4×10^5 turnovers [2]. The rate of formation of the 3(*R*)-enantiomer is still much faster ($>10^6$) than the uncatalyzed rate, which means that formation of this enantiomer is also catalyzed by the enzyme. Interestingly, mutation of E164, one of the catalytic glutamates, does not affect the rate of production of the 3(*R*)-enantiomer but does reduce the rate of catalysis for the 3(*S*)-enantiomer (Table 3). However, mutation of E144 or removal of the hydrogen bonding network through replacement of either G141 or A98 with proline affects the rates of formation for both enantiomers, though not necessarily to the same degree [20]. Modeling studies indicate that the *s-cis* conformer is positioned in the active site to produce the 3(*S*)-enantiomer. If the water molecule that hydrates the *s-cis* conformer is similarly positioned for the *s-trans* conformer, then rotation of 180° about the C1-C2 bond presents the opposite face of the double bond to the water molecule, resulting in formation of the incorrect 3(*R*)-enantiomer. Thus, the presence of two bound conformers provides an explanation for the ability of the enzyme to produce both the 3(*S*)- and 3(*R*)-hydroxybutyryl-CoAs. However, since only the *s-cis* conformer is optimally aligned with the catalytic machinery, preferential hydration of this conformer can explain the stereoselectivity of the enzyme-catalyzed reaction.

Multiple bound conformers may be a common theme in the binding of substrates such as fatty acids to enzymes, since the acyl portion of these molecules lacks functional groups that can interact with the active site and fix the conformation. Liu and colleagues have studied the inactivation of enoyl-CoA hydratase with (methylenecyclopropyl)formyl-CoA (MCPF-CoA) [26]. Interestingly, they demonstrated that the (*R*)- and (*S*)-diastereomers of MCPF-CoA inactivated the enzyme with similar second order rate constants, suggesting that the active site was able to accommodate equally either diastereomer. Fur-

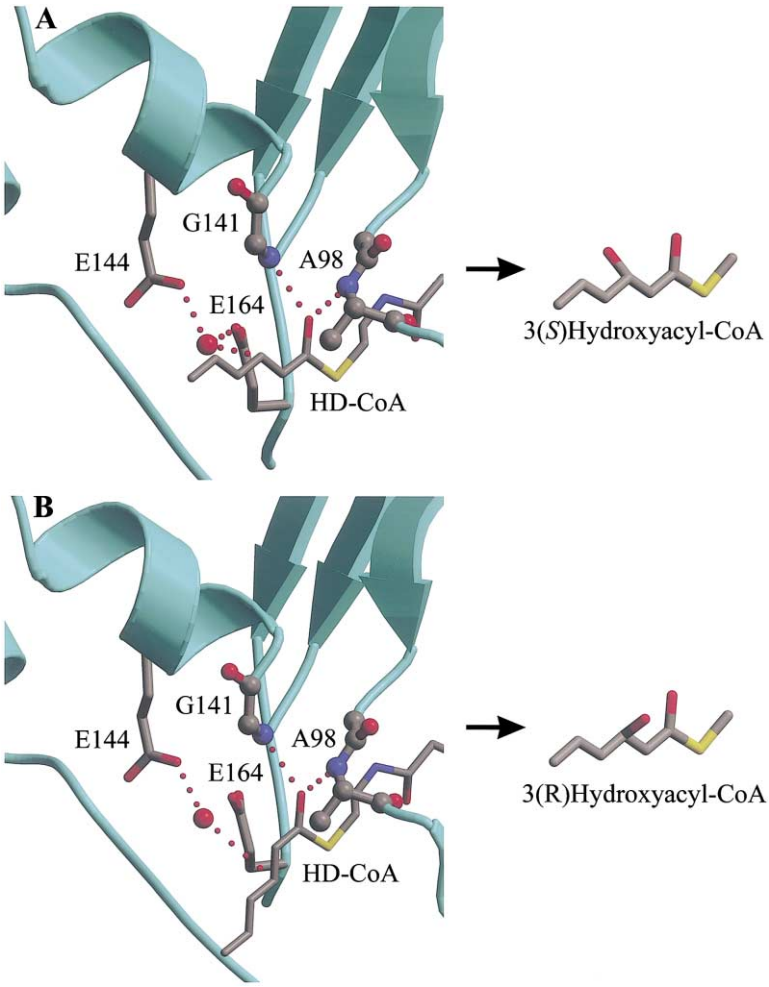

Figure 3. Crystal Structure of Hexadienoyl-CoA Bound to Enoyl-CoA Hydratase

(A) X-ray crystal structure of HD-CoA bound to wild-type enoyl-CoA hydratase. Addition of the water molecule (W48) to the *s-cis* conformer of the ligand will result in the formation of 3(*S*)-hydroxyacyl-CoA (shown schematically). Also shown are the side chains of the two catalytic glutamates (E144 and E164) as well as the two residues (G141 and A98) that comprise the oxyanion hole.

(B) Model of the *s-trans* ligand conformer obtained by rotation of 180° about the hexadienoyl C1-C2 single bond and assuming that the hydrogen bond interactions with the oxyanion hole remain unchanged. If the water molecule that adds to the *s-trans* conformer is in a similar position to that shown for W48, then hydration of the *s-trans* conformer will result in the formation of 3(*R*)-hydroxyacyl-CoA (shown schematically). While the exact location of W48 with respect to the *s-trans* conformer is unknown, the dotted line indicating an interaction between W48 and E144 has been left in place since mutation of E144 affects the rate of forming 3(*R*)-hydroxybutyryl-CoA. These figures were generated with the programs MOLSCRIPT [59] and RASTER3D [60].

thermore, evidence also exists for the presence of multiple ligand populations bound to medium chain acyl-CoA dehydrogenase (MCAD), the enzyme that precedes enoyl-CoA hydratase in the β-oxidation pathway. Our Raman studies suggest similarities in the way in which ligands interact with both enzymes, and Tamaoki et al. have proposed a two-state model for 3-thia-acyl-CoAs of varying chain lengths bound to MCAD using resonance Raman and ^{13}C NMR data [27]. The two distinct forms of the ligand were described as productively and nonproductively bound and represented an anionic form that was able to form a charge transfer complex with the flavin cofactor and a neutral form that could not.

Table 3. Enzymatic Activity and Stereoselectivity of Wild-Type and Mutant Enoyl-CoA Hydratases

Enzyme	k_{cat}[a]	% Activity[b]	k_S/k_R[c]
wt	1790 ± 120	100	4×10^5
E144D[d]	26 ± 1	1.9	ND[e]
E164D	1.50 ± 0.01	0.08	1000
E144Q	0.60 ± 0.01	0.03	$>2.9 \times 10^4$
E164Q	0.0053 ± 0.0003	0.0003	0.33

[a] k_{cat} values for crotonyl-CoA were determined at 25°C in 20 mM (pH 7.4) sodium phosphate buffer containing 3 mM EDTA. Data for the wild-type and E164Q enzymes were taken from Hofstein et al. [12]. Data for E144D, E164D, and E144Q are reported [20].

[b] Activity relative to wild-type enzyme.

[c] Ratio of the rate of product enantiomer formation, determined as described in Wu et al. [2]. Data for the wild-type enzyme are taken from Wu et al. [2] and the data for the mutants are taken from Feng et al. [20].

[d] Data determined with 3′-dephosphocrotonyl-CoA as substrate. Decrease in k_{cat} relative to k_{cat} determined for wild-type enzyme with the same substrate (1380 s^{-1}) [12].

[e] Not determined.

Ground State Effects in Enzyme Catalysis

The enzyme-ligand interactions that result in the observed polarization of the *s-cis* hexadienoyl conformer are electrostatic in origin and cause a distortion of the ligand structure toward the carbanionic transition state predicted for substrate hydration. Consistent with calculations on a similar system [28], we estimate that the 30 cm^{-1} change in the enone vibrational band correlates with a 0.02 Å increase in the hexadienoyl C2=C3 bond length, which is ~10% of the expected change along the reaction coordinate to the transition state if the latter approximates an enolate. Similar evidence for ground state distortion has been provided by vibrational and NMR spectroscopies in other enzyme systems [22, 25, 29–39]. In accordance with the work of Cheng et al. [50],

we believe that these changes in ligand structure result from placing the substrate (analog) in an environment that has evolved to bind the transition state for the reaction rather than the ground state. Consequently the substrate is stressed because it is under pressure to adopt the charge distribution and structure present in the transition state. In response to this stress, the substrate deforms and this deformation is what is classically referred to as ground state strain [40].

While the role of transition state stabilization in enzyme catalysis has long been accepted [41–45], there has been less agreement concerning whether destabilization of the reactant ground state(s) also occurs, and if so, whether it is important for catalysis [40, 46–49]. Consideration of the energetics involved suggests that the strain itself cannot be activating, since deformation would not occur if it were not energetically favorable in comparison to a complex containing the nondeformed substrate. However, deformation of the substrate "costs" a considerable amount of energy. Using computational methods, Anderson and coworkers have estimated that the energy required for ligand polarization in a similar system was 3.2 kcal/mol [28], while analysis of carbonyl stretching frequencies indicates that the strain energy in our system may be up to 7 kcal/mol [14; P.J.T., unpublished]. Since distortion of the substrate carries an energetic cost, the observation of strain constitutes direct evidence that the bound substrate is stressed. The observed ligand polarization, which is the experimental manifestation of the strain, provides information on the vectorial specificity and energetic magnitude of the stress. It is not directed randomly, but along a vector that coincides with the changes in bond length and charge distribution expected for movement along the reaction coordinate. The fact that the most stable state available to the ground state complex is strained implies that the overall interaction energy between enzyme and substrate, of which the strain energy is a component, is lower (and thus the energy of the ground state complex is higher) than it would be if the enzyme were configured so as to be optimally complementary to the unstrained substrate. This energy difference is an example of what has classically been referred to as "ground state destabilization" [40].

Thus, while the strain that we observe is not in itself activating, the observation of substrate strain provides direct evidence for the existence of substrate destabilization. The stress in the ground state that causes the strain acts to destabilize the ground state relative to the transition state and thus lowers the barrier for reaction. Only stress that is directed along the reaction coordinate can achieve this effect, because only then is the stress relieved by the structural changes that occur upon reaching the transition state. The relationship between ground state strain and reactivity in phosphoryl transfer reactions has recently been examined using vibrational spectroscopy [50]. We agree with these authors that strain originates from the specific complementarity of the enzyme of the transition state and does not itself contribute directly to catalysis. Rather, it reflects vectorially specific destabilization that exists in the ground state. The above calculations of strain energy suggest that the ground state destabilization inferred from our results in the enoyl-CoA hydratase system may be responsible for 10^2- to 10^5-fold of the increase in k_{cat} that the enzyme achieves, out of an overall rate increase of $>10^{11}$-fold.

Analysis of the high stereoselectivity of the reaction catalyzed by enoyl-CoA hydratase illustrates the subtle interplay between ground state destabilization, transition state binding, and catalysis in this system. Since hydration of 2-*trans*-crotonyl-CoA leads to preferential formation of the 3(*S*) product enantiomer with a stereospecificity of 400,000 to 1, the transition state leading to 3(*S*)-hydroxybutyryl-CoA must be $\sim$7.6 kcal/mol more stable than the transition state leading to the 3(*R*) enantiomer [51]. Mutational analysis shows that a major contributor to selective stabilization of the transition state for formation of the preferred 3(*S*) product derives from interactions with E164 [20]. Mutation of residues in the oxyanion hole affected the rate of formation of both products; however, because of the low rate of formation of the 3(*R*) product it was not possible to quantitatively compare the effects on the two processes. Analysis of ground state strain effects suggests that interactions with the oxyanion hole also contribute substantially to differential stabilization of the 3(*S*) transition state. The observation that only the *s-cis* hexadienoyl conformer is polarized by the enzyme is entirely consistent with X-ray crystallographic studies indicating that the 3(*S*)-hydroxyacyl-CoA product requires that the substrate be bound in an *s-cis* conformation about the C1-C2 single bond. Consequently, of the two bound substrate populations, only the *s-cis* conformer is productively aligned with interactions that stabilize the 3(*S*) product's transition state, and so only this conformer undergoes ground state destabilization as revealed by ligand polarization. The lack of polarization in the *s-trans* conformer indicates that there is little if any stress on the substrate directed along the reaction coordinate leading to the 3(*R*) product. Thus, while the presence of strain in the *s-cis* complex is not in itself responsible for the stereoselectivity of the reaction, it signals the contribution to stereoselectivity made by specific interactions that promote charge reorganization leading to the transition state for the 3(*S*) product compared to that producing the 3(*R*) enantiomer.

Significance

Vibrational spectroscopy is a powerful method for probing the intimate details of enzyme catalysis. It operates on a time scale that is much faster than molecular motions, thereby providing a snapshot of all structures present at any instant. Moreover, the vibrational spectrum is exquisitely sensitive to perturbations in the structure of the bound ligand and can thus report directly on catalytically important enzyme-substrate interactions. In the present example, the observation of two bound hexadienoyl conformers, only one of which is activated, can be used to rationalize the stereoselectivity of the enzyme-catalyzed reaction, and additionally sheds light on the origins of catalysis by this enzyme. The polarization of the *s-cis* hexadienoyl conformer is an example of ground state strain arising from the selective comple-

mentarity of the enzyme toward the transition state rather than the ground state. The net interaction energy between enzyme and substrate will increase in the transition state, as the accompanying charge separation and structural changes result in increased complementarity with the enzyme and thus to stronger binding and to the relief of energetically costly strain [52]. This increase in the net interaction energy between enzyme and substrate stabilizes the transition state relative to the ground state. Thus, while stabilization of the transition state is solely responsible for increasing k_{cat}/K_M, destabilization of the ground state is important for achieving a high k_{cat} [40]. The structural change that accompanies ligand polarization is a relatively small distortion along the reaction coordinate toward the transition state. However, by indicating the existence of stresses on the substrate and by providing information on their strength and on their vectorial specificity with respect to the reaction coordinate, experimental observations of ground state strain provide precise information on interactions in the ground state that contribute to catalysis.

Experimental Procedures

Ligand Synthesis, Protein Expression, and Purification

Hexadienoyl-imidazole was prepared from hexadienoic acid and 1,1-carbonyl-diimidazole as described [16]. Hexadienoyl-CoA (HD-CoA) was synthesized from hexadienoyl-imidazole and CoA as described [14]. Recombinant wild-type rat mitochondrial enoyl-CoA hydratase was expressed and purified from cultures of *E. coli* as described [12, 19]. The E164Q and E144Q mutants were available from a previous study while the E164D and E144D mutants were constructed using QuikChange Mutagenesis (Stratagene) [12]. Following affinity purification on a CoA-sepharose column, the enzymes were concentrated to 0.8–1 mM active sites using a centricon-10 (Amicon).

Synthesis and Crystallographic Studies of S-Hexadienoyl-N-Acetylcysteamine (HD-NAC)

Hexadienoyl-imidazole (0.2 g, 1.2 mmol) was dissolved in 5 ml of dry THF, and 0.15 g (1.3 mmol) of N-acetylcysteamine was added. The solution was stirred for 30 min and the resulting product was purified by preparative reverse-phase HPLC using 0.2 M $NH_4^+CH_3COO^-$/1.75% acetonitrile as buffer A and running a 0%–100% gradient of acetonitrile in 40 min. The HPLC run was monitored at 285 and 330 nm and fractions containing HD-NAC (28 min elution time) were pooled and lyophilized. UV (H_2O) λ_{max} 295 nm, ϵ_{295} 10,000 M^{-1} cm^{-1}. ^1H NMR ($CDCl_3$) δ 7.20 (dd, 1H, J_{trans} = 15.5 Hz, ^3J = 10.0), 6.26 (dq, 1H, J_{trans} = 16.4 Hz, ^3J = 7.5), 6.16 (dd, 1H, J_{trans} = 16.4 Hz, ^3J = 10.0), 6.08 (d, 1 H, J_{trans} = 15.5 Hz), 5.92 (b, 1H, NH), 3.47 (m, 2H), 3.11 (t, 2H, ^3J = 6.3 Hz), 1.96 (s, 3H), 1.87 (d, 3H, ^3J = 7.5 Hz). HRMS (ESI): m/z calculate for $C_{10}H_{15}NO_2S$, 213.0824; found, 213.0818. Crystals of HD-NAC were grown from an aqueous solution of HD-NAC initially dissolved at 100°C in H_2O and allowed to cool slowly to RT. The X-ray crystal structure was solved using an Enraf-Nonius diffractometer. Selected torsion angles: O-C1-C2-C3, 164.7° (*s-trans*); C1-C2-C3-C4, 178.1° (*trans*); C2-C3-C4-C5, 177.5° (*s-trans*); C3-C4-C5-C6, 179.2° (*trans*); O-C1-S-C7, 1°.

Raman Spectroscopy

Raman difference spectra were acquired using 700 mW 752 nm laser excitation as described previously [14]. For single-crystal Raman spectroscopy, crystals of HD-NAC were mounted on a needle. For the enzyme-ligand spectra, Raman intensities were calibrated against a Raman spectrum of cyclohexanone and then corrected for concentration and acquisition time. Using this method the intensity data has an error of approximately ±10%.

Crystallization, Structure Determination, and Refinement

Crystals of wild-type enoyl-CoA hydratase were grown at 22°C by vapor diffusion in hanging drops containing 1 μl of protein solution (100 μM protein and 1 mM HD-CoA) and 1 μl of reservoir solution containing 2.4 M $(NH_4)_2SO_4$, 1 mM DTT, 1 mM EDTA, 5% n-octanol, and 100 mM MES (pH 6.5). The crystals belong to space group $P2_12_12_1$ with unit cell dimensions a = 76.9 Å, b = 95.2 Å, c = 249.4 Å. Given the crystal lattice, there is one homohexamer in the asymmetric unit. Diffraction data were collected from cryocooled crystals soaked in mother liquor containing 25% (v/v) glycerol. Diffraction data were collected at a wavelength of 1.1 Å at the National Synchrotron Light Source at Brookhaven National Laboratory. Data were indexed, integrated, and scaled using HKL [53]. The enoyl-CoA hydratase structure bound to HD-CoA was solved by difference Fourier methods utilizing the refined coordinates from the 2.5 Å structure of enoyl-CoA hydratase with the competitive inhibitor acetoacetyl-CoA bound (PDB entry 1DUB). The model utilized for the difference Fourier calculation was the hexamer without the bound inhibitor. Refinement of this model was performed using REFMAC5 [54] along with amplitudes to 2.1 Å resolution with the inclusion of tight non-crystallographic restraints between all subunits within the asymmetric unit except subunit D, which contained no HD-CoA ligand. The final rounds of refinement were performed with relaxed noncrystallographic restraints. All model manipulation and side chain positioning was performed using the program O [55]. The program ARP [56] was used to build the solvent structure into the resulting density maps. Geometry was assessed with PROCHECK [57]. For subsequent calculations the CCP4 suite was utilized [58]. Data collection and refinement statistics are given in Table 2.

Acknowledgments

This work was supported in part by grants from NIH (AI44639 and GM63121) and NSF (MCB9604254) to P.J.T. In addition, this material is based upon work supported in part by the U.S. Army Research Office under grant DAAG55-97-1-0083 to P.J.T. P.J.T. is an Alfred P. Sloan Research Fellow. A.F.B. was supported by an American Heart Association postdoctoral fellowship. S.P. was supported by a DOE/GAANN fellowship. The NMR facility at SUNY Stony Brook is supported by grants from NSF (CHE9413510) and NIH (1S10RR554701).

Received: July 8, 2002
Revised: October 3, 2002
Accepted: October 3, 2002

References

1. Willadsen, P., and Eggerer, H. (1975). Substrate stereochemistry of the enoyl-CoA hydratase reaction. Eur. J. Biochem. *54*, 247–252.
2. Wu, W.J., Feng, Y., He, X., Hofstein, H.A., Raleigh, D.P., and Tonge, P.J. (2000). Stereospecificity of the reaction catalyzed by enoyl-CoA hydratase. J. Am. Chem. Soc. *122*, 3987–3994.
3. Gerlt, J.A., and Babbitt, P.C. (2001). Divergent evolution of enzyme function: mechanistically diverse superfamilies and functionally distinct suprafamilies. Annu. Rev. Biochem. *70*, 209–246.
4. Holden, H.M., Benning, M.M., Haller, T., and Gerlt, J.A. (2001). The crotonase superfamily: divergently related enzymes that catalyze different reactions involving acyl coenzyme a thioesters. Acc. Chem. Res. *34*, 145–157.
5. Engel, C.K., Mathieu, M., Zeelen, J.P., Hiltunen, J.K., and Wierenga, R.K. (1996). Crystal structure of enoyl-coenzyme A (CoA) hydratase at 2.5 angstroms resolution: a spiral fold defines the CoA-binding pocket. EMBO J. *15*, 5135–5145.
6. Engel, C.K., Kiema, T.R., Hiltunen, J.K., and Wierenga, R.K. (1998). The crystal structure of enoyl-CoA hydratase complexed with octanoyl-CoA reveals the structural adaptations required for binding of a long chain fatty acid-CoA molecule. J. Mol. Biol. *275*, 847–859.
7. Bahnson, B.J., Anderson, V.E., and Petsko, G.A. (2002). Structural mechanism of enoyl-CoA hydratase: three atoms from a

single water are added in either an E1cb stepwise or concerted fashion. Biochemistry *41*, 2621–2629.
8. Bahnson, B.J., and Anderson, V.E. (1989). Isotope effects on the crotonase reaction. Biochemistry *28*, 4173–4181.
9. Bahnson, B.J., and Anderson, V.E. (1991). Crotonase-catalyzed beta-elimination is concerted: a double isotope effect study. Biochemistry *30*, 5894–5906.
10. D'Ordine, R.L., Bahnson, B.J., Tonge, P.J., and Anderson, V.E. (1994). Enoyl-coenzyme A hydratase-catalyzed exchange of the α-protons of coenzyme A thiol esters: a model for an enolized intermediate in the enzyme-catalyzed elimination? Biochemistry *33*, 14733–14742.
11. Muller-Newen, G., Janssen, U., and Stoffel, W. (1995). Enoyl-CoA hydratase and isomerase form a superfamily with a common active-site glutamate residue. Eur. J. Biochem. *228*, 68–73.
12. Hofstein, H.A., Feng, Y., Anderson, V.E., and Tonge, P.J. (1999). Role of glutamate 144 and glutamate 164 in the catalytic mechanism of enoyl-CoA hydratase. Biochemistry *38*, 9508–9516.
13. Kiema, T.R., Engel, C.K., Schmitz, W., Filppula, S.A., Wierenga, R.K., and Hiltunen, J.K. (1999). Mutagenic and enzymological studies of the hydratase and isomerase activities of 2-enoyl-CoA hydratase-1. Biochemistry *38*, 2991–2999.
14. Bell, A.F., Wu, J., Feng, Y., and Tonge, P.J. (2001). Importance of G141 in substrate polarization by enoyl-CoA hydratase. Biochemistry *40*, 1725–1733.
15. D'Ordine, R.L., Tonge, P.J., Carey, P.R., and Anderson, V.E. (1994). Electronic rearrangement induced by substrate analog binding to the enoyl-CoA hydratase active site: evidence for substrate activation. Biochemistry *33*, 12635–12643.
16. Tonge, P.J., Anderson, V.E., Fausto, R., Kim, M., PusztaiCarey, M., and Carey, P.R. (1995). Localized electron polarization in a substrate analog binding to the active site of enoyl-CoA hydratase: Raman spectroscopic and conformational analyses of rotamers of hexadienoyl thiolesters. Biospectroscopy *1*, 387–394.
17. Fausto, R., Tonge, P.J., and Carey, P.R. (1994). Molecular structures of *cis*-S-ethyl and *trans*-S-ethyl thiocrotonate—a combined vibrational spectroscopic and *ab-initio* SCF-MO study. J. Chem. Soc. Faraday Trans. *90*, 3491–3503.
18. Person, W.B., and Zerbi, G. (1982). Vibrational intensities in infrared and Raman spectroscopy (Amsterdam: Elsevier).
19. Wu, W.J., Anderson, V.E., Raleigh, D.P., and Tonge, P.J. (1997). Structure of hexadienoyl-CoA bound to enoyl-CoA hydratase determined by transferred nuclear Overhauser effect measurements: mechanistic predictions based on the X-ray structure of 4-(chlorobenzoyl)-CoA dehalogenase. Biochemistry *36*, 2211–2220.
20. Feng, Y., Hofstein, H., Zwahlen, J., and Tonge, P.J. (2002). Effect of mutagenesis on the stereochemistry of the reaction catalyzed by enoyl-CoA hydratase. Biochemistry *41*, 12883–12890.
21. Clarkson, J., Tonge, P.J., Taylor, K.L., Dunaway-Mariano, D., and Carey, P.R. (1997). Raman study of the polarizing forces promoting catalysis in 4-chlorobenzoate-CoA dehalogenase. Biochemistry *36*, 10192–10199.
22. Taylor, K.L., Xiang, H., Liu, R.Q., Yang, G., and Dunaway-Mariano, D. (1997). Investigation of substrate activation by 4-chlorobenzoyl-coenzyme A dehalogenase. Biochemistry *36*, 1349–1361.
23. Dong, J., Xiang, H., Luo, L., Dunaway-Mariano, D., and Carey, P.R. (1999). Modulating electron density in the bound product, 4-hydroxybenzoyl-CoA, by mutations in 4-chlorobenzoyl-CoA dehalogenase near the 4-hydroxy group. Biochemistry *38*, 4198–4206.
24. Luo, L.S., Taylor, K.L., Xiang, H., Wei, Y.S., Zhang, W.H., and Dunaway-Mariano, D. (2001). Role of active site binding interactions in 4-chlorobenzoyl-coenzyme A dehalogenase catalysis. Biochemistry *40*, 15684–15692.
25. Dinakarpandian, D., Shenoy, B.C., Hilvert, D., McRee, D.E., McTigue, M., and Carey, P.R. (1999). Electric fields in active sites: substrate switching from null to strong fields in thiol- and selenol-subtilisins. Biochemistry *38*, 6659–6667.
26. Dakoji, S., Li, D., Agnihotri, G., Zhou, H.Q., and Liu, H.W. (2001). Studies on the inactivation of bovine liver enoyl-CoA hydratase by (methylenecyclopropyl)formyl-CoA: elucidation of the inactivation mechanism and identification of cysteine-114 as the entrapped nucleophile. J. Am. Chem. Soc. *123*, 9749–9759.
27. Tamaoki, H., Nishina, Y., Shiga, K., and Miura, R. (1999). Mechanism for the recognition and activation of substrate in medium-chain acyl-CoA dehydrogenase. J. Biochem. (Tokyo) *125*, 285–296.
28. D'Ordine, R.L., Pawlak, J., Bahnson, B.J., and Anderson, V.E. (2002). Polarization of cinnamoyl-CoA substrates bound to enoyl-CoA hydratase: correlation of 13C NMR with quantum mechanical calculations and calculation of electronic strain energy. Biochemistry *41*, 2630–2640.
29. Belasco, J.G., and Knowles, J.R. (1980). Direct observation of substrate distortion by triosephosphate isomerase using Fourier transform infrared spectroscopy. Biochemistry *19*, 472–477.
30. Belasco, J.G., and Knowles, J.R. (1983). Polarization of substrate carbonyl groups by yeast aldolase: investigation by Fourier transform infrared spectroscopy. Biochemistry *22*, 122–129.
31. Kurz, L.C., Ackerman, J.J., and Drysdale, G.R. (1985). Evidence from 13C NMR for polarization of the carbonyl of oxaloacetate in the active site of citrate synthase. Biochemistry *24*, 452–457.
32. Tonge, P.J., and Carey, P.R. (1992). Forces, bond lengths, and reactivity: fundamental insight into the mechanism of enzyme catalysis. Biochemistry *31*, 9122–9125.
33. Nishina, Y., Sato, K., Shiga, K., Fujii, S., Kuroda, K., and Miura, R. (1992). Resonance Raman study on complexes of medium-chain acyl-CoA dehydrogenase. J. Biochem. (Tokyo) *111*, 699–706.
34. Burke, J.R., and Frey, P.A. (1993). The importance of binding energy in catalysis of hydride transfer by UDP-galactose 4-epimerase: a 13C and 15N NMR and kinetic study. Biochemistry *32*, 13220–13230.
35. Austin, J.C., Fitzhugh, A., Villafranca, J.E., and Spiro, T.G. (1995). Stereoelectronic activation of methylenetetrahydrofolate by thymidylate synthase: resonance Raman spectroscopic evidence. Biochemistry *34*, 7678–7685.
36. Austin, J.C., Zhao, Q., Jordan, T., Talalay, P., Mildvan, A.S., and Spiro, T.G. (1995). Ultraviolet resonance Raman spectroscopy of delta 5–3-ketosteroid isomerase revisited: substrate polarization by active-site residues. Biochemistry *34*, 4441–4447.
37. Carey, P.R. (1998). Raman spectroscopy in enzymology: the first 25 years. J. Raman Spec. *29*, 7–14.
38. Deng, H., and Callender, R. (1999). Raman spectroscopic studies of the structures, energetics, and bond distortions of substrates bound to enzymes. Methods Enzymol. *308*, 176–201.
39. Wilkinson, A.S., Ward, S., Kania, M., Page, M.G.P., and Wharton, C.W. (1999). Multiple conformations of the acylenzyme formed in the hydrolysis of methicillin by *Citrobacter freundii* beta-lactamase: a time-resolved FTIR spectroscopic study. Biochemistry *38*, 3851–3856.
40. Jencks, W.P. (1975). Binding energy, specificity, and enzymic catalysis: the circe effect. Adv. Enzymol. Relat. Areas Mol. Biol. *43*, 219–410.
41. Pauling, L. (1946). Molecular architecture and biological reactions. Chem. Eng. News *24*, 1375–1377.
42. Fersht, A. (1998). Structure and mechanism in protein science: a guide to enzyme catalysis and protein folding (New York: W.H. Freeman).
43. Schramm, V.L., Horenstein, B.A., and Kline, P.C. (1994). Transition state analysis and inhibitor design for enzymatic reactions. J. Biol. Chem. *269*, 18259–18262.
44. Bruice, T.C., and Benkovic, S.J. (2000). Chemical basis for enzyme catalysis. Biochemistry *39*, 6267–6274.
45. Wolfenden, R., and Snider, M.J. (2001). The depth of chemical time and the power of enzymes as catalysts. Acc. Chem. Res. *34*, 938–945.
46. Narlikar, G.J., Gopalakrishnan, V., McConnell, T.S., Usman, N., and Herschlag, D. (1995). Use of binding energy by an RNA enzyme for catalysis by positioning and substrate destabilization. Proc. Natl. Acad. Sci. USA *92*, 3668–3672.
47. Warshel, A., Strajbl, M., Villa, J., and Florian, J. (2000). Remarkable rate enhancement of orotidine 5′-monophosphate decarboxylase is due to transition-state stabilization rather than to ground-state destabilization. Biochemistry *39*, 14728–14738.
48. Warshel, A., Florian, J., Strajbl, M., and Villa, J. (2001). Circe

effect versus enzyme preorganization: what can be learned from the structure of the most proficient enzyme? Chembiochem *2*, 109–111.

49. Miller, B.G., Butterfoss, G.L., Short, S.A., and Wolfenden, R. (2001). Role of enzyme-ribofuranosyl contacts in the ground state and transition state for orotidine 5′-phosphate decarboxylase: a role for substrate destabilization? Biochemistry *40*, 6227–6232.
50. Cheng, H., Nikolic-Hughes, I., Wang, J.H., Deng, H., O'Brien, P.J., Wu, L., Zhang, Z.Y., Herschlag, D., and Callender, R. (2002). Environmental effects on phosphoryl group bonding probed by vibrational spectroscopy: implications for understanding phosphoryl transfer and enzymatic catalysis. J. Am. Chem. Soc. *124*, 11295–11306.
51. Seeman, J.I. (1983). Effect of conformational change on reactivity in organic chemistry. Evaluations, applications, and extensions of Curtin-Hammett Winstein-Holness kinetics. Chem. Rev. *83*, 83–134.
52. Shan, S.O., and Herschlag, D. (1996). The change in hydrogen bond strength accompanying charge rearrangement: implications for enzymatic catalysis. Proc. Natl. Acad. Sci. USA *93*, 14474–14479.
53. Otwinowski, Z., and Minor, W. (1997). Processing of X-ray diffraction data collected in oscillation mode. In Methods Enzymol., Volume 276, C.W. Carter and R.M. Sweet, eds. (New York: Academic Press), pp. 307–326.
54. Murshudov, G.N., Vagin, A.A., and Dodson, E.J. (1997). Refinement of macromolecular structures by the maximum-likelihood method. Acta Crystallogr. D *53*, 240–255.
55. Jones, T.A., Zou, J.Y., Cowan, S.W., and Kjeldgaard, M. (1991). Improved methods for building protein models in electron-density maps and the location of errors in these models. Acta Crystallogr. A *47*, 110–119.
56. Perrakis, A., Morris, R., and Lamzin, V.S. (1999). Automated protein model building combined with iterative structure refinement. Nat. Struct. Biol. *6*, 458–463.
57. Laskowski, R.A., Macarthur, M.W., Moss, D.S., and Thornton, J.M. (1993). Procheck—a program to check the stereochemical quality of protein structures. J. Appl. Crystallogr. *26*, 283–291.
58. CCP4 (Collaborative Computational Project 4) (1994). The CCP4 suite: programs for protein crystallography. Acta Crystallogr. D *50*, 760–763.
59. Kraulis, P.J. (1991). Molscript—a program to produce both detailed and schematic plots of protein structures. J. Appl. Crystallogr. *24*, 946–950.
60. Merritt, E.A., and Murphy, M.E.P. (1994). Raster3d version-2.0—a program for photorealistic molecular graphics. Acta Crystallogr. D *50*, 869–873.